Intelligent UAV Swarm Coexistence in DTV Bands

Rajrshi Dubey, Ashutosh Balakrishnan, and Swades De,
Department of Electrical Engineering and Bharti School of Telecommunications, Indian Institute of Technology Delhi, India
rajrshi.dubey@iitd.ac.in, ashutosh.balakrishnan@iitd.ac.in, swadesd@iitd.ac.in

***Abstract*—Intelligent spectrum sharing is one of the key enablers of upcoming sixth generation (6G) communications. Unmanned aerial vehicles (UAVs) have emerged as an attractive low altitude aerial base station (BS), providing on demand capacity especially in urban areas. This work aims to demonstrate the feasibility of coexisting UAV to UAV communication based adhoc network over digital television (DTV) bands governed through latest ATSC 3.0 standards. We propose an adaptive modulation and dynamic subcarrier (AMDS) allocation framework to intelligently allocate the resources at the UAV network through adaptive bit loading and frequency allocations. The work aims to maximize the capacity of the coexisting UAV network in addition to protecting the performance of the TV-receiver from the resultant coexisting network interference. A rate maximization problem is formulated and solved using a low computation complexity based bi-section method. Extensive simulation results indicate that the connected UAV link can achieve up to 40 Mbps capacity when 1 km apart, while coexisting and guaranteeing the performance of the DTV network.**

***Index Terms*—Coexistence, UAV, DTV, adaptive modulation, ATSC 3.0, spectrum sharing**

I. Introduction

Efficient spectrum usage has emerged as a key requirement in designing future networks with continually growing data requirements towards sixth generation (6G) communications [1]. While higher frequency bands in mmWave and tera-hertz frequencies are being proposed to cater to increasing user quality of service (QoS) requirements, these bands are prone to much higher path loss. Coexisting the cellular communication on digital television (DTV) bands has been an interesting prospect towards improving the spectral efficiency [2]. Furthermore, 6G technologies include deployment of unmanned aerial vehicles (UAV) based adhoc communication networks facilitating on-demand additional capacity injection in the network. The UAV act as low altitude aerial base stations (BS) and are extremely useful in providing telecommunication access in disaster scenarios, utility applications like automated delivery service in urban cities, and industrial areas [3].

There have been ongoing efforts towards coexisting the traditional cellular network with DTV bands as in [4]–[8]. With television going digital, Advanced Television Systems Committee (ATSC) has proposed ATSC 3.0 standards for enhancing user experience in DTV [9]. In this paper we explore coexistence of UAV swarm, i.e., a group of UAVs, in ATSC 3.0 based DTV bands. The aim of the paper is to maximize the capacity of the coexisting UAV network while also guaranteeing the QoS of DTV network. An adaptive modulation and dynamic subcarrier (AMDS) framework is proposed to intelligently allocate resources to the UAV network while protecting the TV receiver performance from the resulting interference. The key contributions are as follows.

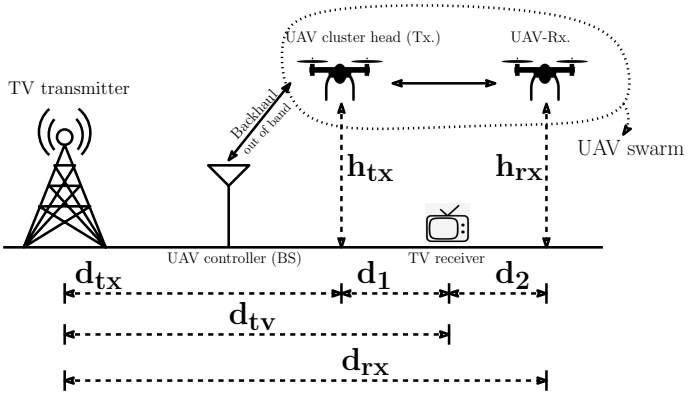

Figure 1: Proposed system model.

A. Contributions

(1) We present an analytical framework demonstrating the feasibility of UAV network coexistence in ATSC 3.0 based DTV frequency bands. (2) The primary aim is to maximize the UAV network data rate, while protecting the performance of TV-receiver from the interference arising from coexistence. (3) An AMDS framework is proposed to intelligently allocate the UAV transmission parameters namely, modulation constellation and frequency subcarriers, through adaptive bit loading and dynamic frequency allocation. With the average SINR denoting QoS of TV-receiver, the AMDS framework ensures protection of the TV receiver from spectrum sharing interference. (4) A rate maximization problem is formulated and solved using bi-section method, having much lower complexity than the traditional exhaustive search method. (5) Our results demonstrate that the connected UAVs can achieve up to 40 Mbps capacity when 1 km apart, while coexisting and maintaining the DTV network performance.

II. System Model

In this work, we analyze a UAV to UAV communication network coexisting together with a TV-trasmitter (TV-Tx.) and its corresponding TV-receiver (TV-Rx.). The TV-Tx is assumed to be located at the center of the TV coverage area. A TV-Rx is assumed to be within the TV coverage area, receiving the TV signals. The paper assumes a swarm of UAVs operating in the TV coverage area. While the analysis can be generalized for any number of UAVs, this paper performs the coexistence study in a two UAV scenario. The

UAV communicate with each other such that the UAV-cluster head (or UAV-Transmitter, UAV-Tx.) communicates with the UAV-receiver (UAV-Rx.), interfering with the DTV network. It may be noted that the UAV-Tx and cluster head are used interchangeably in the paper.

The swarm of UAVs are controlled by a BS through the cluster head. The backhaul between the cluster head and the other BS is assumed to be out-of-band and not in the DTV bands, hence not interfering with the UAV communication or TV-Rx signal reception. The UAV cluster head communicates with the other UAVs in the TV broadcast band, coexisting with the TV-Rx signals as shown in Fig. 1. The UAV channel is modelled as per 3GPP standards, with the average path loss given by $PL^{(U)} = (p_{LoS}PL_{LoS} + p_{NLoS}PL_{NLoS})$. Here, $P_{LoS}, P_{NLoS}, p_{LoS}$, and p_{LoS} respectively represent the Line-of-sight (LoS) and non-LoS path loss components and their corresponding probabilities [10].

Let h_{tx} and d_{tx} represent the height of UAV-Tx, and the distance between the TV-Tx and the UAV-Tx, respectively. The UAV-Rx is present at a distance of d_{rx} from the TV-Tx and flying at the height of h_{rx} from the ground. Let $d_1 = d_{TV} - d_{tx}$ and $d_2 = d_{rx} - d_{TV}$, respectively denote the distance between UAV-Tx and UAV-Rx with the TV-Rx. In the upcoming section, we present the signaling model of the DTV and UAV network in addition to the receiver signal models.

III. Signal Modelling and Interference Analysis

A. DTV signalling model

The upcoming TV technologies like ATSC 3.0 uses an orthogonal frequency division multiplexing (OFDM) based waveform to broadcast its data. Let $T_u^{(D)}$, $T_g^{(D)}$, $T^{(D)} = T_u^{(D)} + T_g^{(D)}$, and $\Delta f^{(D)} = \left(1/T_u^{(D)}\right)$, respectively, represent the useful part, guard duration, total symbol duration, and subcarrier spacing of the OFDM waveform used by the TV transmitter. The number of active TV subcarriers is denoted by $N^{(D)}$. It is assumed that the TV-Tx is transmitting with uniform transmit power of $P^{(D)}$ per subcarrier. The signal transmitted by the TV-Tx is given as,

$$x^{(D)}(t) = \sqrt{\frac{P^{(D)}}{T_u^{(D)}}} \sum_{l' \in \mathcal{Z}} \sum_{k'=0}^{N^{(D)}-1} X_{k'}^{(D)}[l'] \times e^{\frac{j2\pi k' t}{T_u^{(D)}}} \Pi\left(\frac{t - l' T_u^{(D)} + T_g^{(D)}}{T^{(D)}}\right). \quad (1)$$

Here, the variable k' represents the subcarrier index, l' denotes the OFDM symbol index, $X_{k'}^{(D)}$ represents the digitally modulated symbol transmitted by the TV transmitter on the k'-th subcarrier. The modulated symbols are assumed to be of unit energy i.e., $\mathbb{E}[|X_{k'}^{(D)}|^2] = 1 \; \forall \; k' \in \{0, 1, \ldots, N^{(D)} - 1\}$. Here $\mathbb{E}$ denotes the statistical expectation operator and $\Pi(t)$ represents the pulse shaping function, such that $\Pi(t) = 1$ for $0 \leq t \leq 1$ and 0 otherwise. Assuming the TV signal passes through a multipath channel with L' taps, the TV signal received by the TV-Rx is given as, $s^{(D)}(t) = \sqrt{l^{(Dt)}} x^{(D)}(t) * \sum_{n'=1}^{L'} \delta(t - \tau_{n'}^{(D)})$, with $(*)$ denoting linear convolution operator. $h_{n'}^{(D)}$, $\tau_{n'}^{(D)}$ and $l^{(Dt)}$ represent the complex gaussian channel gain, path delay of the n'-th path of the multipath channel, and path loss experienced by the TV signal between TV-Tx and TV-Rx, respectively.

B. UAV signalling model

The transmit waveform of UAV-Tx is also assumed to be an OFDM-based waveform. $T_u^{(U)}$, $T_g^{(U)}$, $T^{(U)} = T_u^{(U)} + T_g^{(U)}$, and $\Delta f^{(U)} = \left(1/T_u^{(U)}\right)$, respectively, denote the same set of parameters for UAV OFDM waveform, as in DTV signal model. The UAV communicate with each other using frequency division duplexing (FDD). The UAV-Tx utilizes the DTV band for transmitting its data to the UAV-Rx, while the UAV-Rx to UAV-Tx communication occurs over a different, non-overlapping frequency band. The UAV-Tx transmitted signal is given by,

$$x^{(U)}(t) = \sqrt{\frac{1}{T_u^{(U)}}} \sum_{l \in \mathcal{Z}} \sum_{k=0}^{F-1} \sqrt{P^{(U)}} \sum_{n=1}^{L} X_k[l] e^{\frac{j2\pi k t}{T_u^{(U)}}} \times \Pi\left(\frac{t - l T_u^{(U)} + T_g^{(U)}}{T^{(U)}}\right). \quad (2)$$

Here, k represents the subcarrier index, and $F \in \{1, 2, \ldots, N^{(U)}\}$ denotes the number of allocated subcarriers. $N^{(U)}$ represents the maximum number of subcarriers available at the UAV-Tx. $P^{(U)}$ and $X_k[l]$ respectively represent the power and digital symbol transmitted by UAV-Tx over its k-th subcarrier. The variable l denotes the OFDM symbol index. The digital symbols X_k, each of unit power, are selected from the set, $\theta = \{\text{QPSK}, 16-\text{QAM}, 64-\text{QAM}, 256-\text{QAM}\}$. The number of bits per symbol (bit loading per symbol) for an M-QAM symbol is, $b = \log_2 M$. Thus, the set of bit loadings available at UAV-Tx for data transmission is $\chi = \{2, 4, 6, 8\}$. The UAV-Tx signal received by UAV-Rx is given by, $s^{(U)}(t) = \sqrt{l^{(Ur)}} x^{(U)}(t) * \sum_{n=1}^{L} \delta(t - \tau_n^{(U)})$. Here, $h_n^{(U)}$, $\tau_n^{(U)}$, L and $l^{(Ur)}$ respectively represent the complex gaussian channel coefficient, path delay, total multipath components, and the path loss experienced by the UAV signal.

C. DTV receiver model

Let $\mathbf{B}_{\mathbf{p'}}^{(\mathbf{D})}(t) = \left(e^{\frac{-j2\pi p' t}{T_u^{(D)}}} / T_u^{(D)}\right) \Pi\left(\frac{t - l' T_u^{(D)}}{T^{(D)}}\right)$ represent the OFDM basis function of the p'-th subcarrier at the TV-Rx. The signal received at the TV-Rx, after performing the FFT operation over the p'-th subcarrier, is given by $Y_{p'}^{(D)} = \sqrt{P^{(D)}} H_{p'}^{(D)} X_{p'}^{(D)} + U_{p'}$. Here, $H_{p'} = \sum_{n'=1}^{L'} h_{n'}^{(D)} e^{\frac{-j2\pi p' \tau_{n'}^{(D)}}{T_u^{(D)}}}$ denotes the channel frequency response over the p'-th subcarrier. $U_{p'} = \int s^{(U)}(t) B_{p'}^{(D)}(t) dt$ denotes the interference received from the UAV transmission over the p'-th TV subcarrier. The interference power received on the p' subcarrier of TV-Rx is given by,

$$I_{p'} = \mathbb{E}[|U_{p'}|^2] = \int_{p'\Delta f^{(A)} - \frac{\Delta f^{(A)}}{2}}^{p'\Delta f^{(A)} + \frac{\Delta f^{(A)}}{2}} \mathbb{E}\left[|H_k^{(U)}|^2\right] \phi^{(U)}(f) df. \quad (3)$$

Here, $\phi^{(U)}$ represents the power spectral density (PSD) of the UAV transmitted signal [11], which is given as

$$\phi^{(U)} = \sum_{k=0}^{F-1} P^{(U)} T^{(G)} \left(\frac{\sin\left(\pi(f - k\Delta f^{(G)}) T^{(G)}\right)}{\pi(f - k\Delta f^{(G)}) T^{(G)}}\right)^2. \quad (4)$$

Denoting N_0 to represent the PSD of the additive white gaussian noise (AWGN) and $l^{(Ut)}$ to represent the path loss between UAV and TV-Rx link, the resultant SINR over the p'-th TV subcarrier of the TV-Rx is given by, $\gamma_{p'}^{(D)} = P^{(D)} l^{(Dt)} \mathbb{E}[|H_{p'}^{(D)}|^2] / \left(l^{(Ut)} I_{p'} + N_0 \Delta f^{(D)} \right)$.

D. UAV receiver model

The UAV-Rx is assumed to be equipped with an interference cancellation (IC) module to cancel the interference from the TV-Tx. The IC module first decodes the TV signal by assuming the UAV signal as additive noise and then cancels it from the received signal. The residual signal is then processed for decoding the UAV-Tx data. Therefore, the UAV-Tx signal acts as interference to the IC module. Denoting the $\gamma_{p'}^{(U)}$ to represent the SINR of the TV signal over the p'-th subcarrier in the IC module,

$$\gamma_{p'}^{(U)} = \frac{P^{(D)} l^{(Dr)} \mathbb{E}[|H_{p'}^{(D)}|^2]}{l^{(Ur)} I_{p'} + N_0 \Delta f^{(D)}}. \tag{5}$$

Here, the $l^{(Dr)}$ and $l^{(Ur)}$ respectively represent the path loss between the TV-Tx and UAV receiver link and the UAV transmitter and UAV receiver link. Assuming perfect interference cancellation at the IC module, the SINR of the UAV signal over the p-th subcarrier after performing the interference cancellation step is given by, $\Gamma_p^{(U)} = \left(P^{(U)} l^{(Ur)} \mathbb{E}[|H_p^{(U)}|^2] / N_0 \Delta f^{(U)} \right)$. Here, $H_p^{(U)} = \sum_{n=1}^{L} h_n^{(D)} \exp\left(\frac{-j 2\pi p' \tau_n^{(U)}}{T_u^{(U)}} \right)$ denotes the channel frequency response experienced by the UAV-Tx signal at the p-th subcarrier of the UAV-Rx. It may be noted that we have not assumed any IC module in the TV-Rx and hence the UAV has to adjust its transmission parameters to control the interference at the TV-Rx. In the upcoming section, we explain the problem formulation and the proposed AMDS based solution.

IV. Problem Formulation

The resource allocation problem $(P1)$ aims to determine the UAV transmission parameters namely the modulation format/bit loading (x), number of subcarriers (F), and transmit power $P^{(U)}$, to maximize the UAV link throughput, while also protecting the QoS of the TV-Rx. The QoS of the TV-Rx is given by the mean SINR of the TV signal at the TV-Rx i.e., $\bar{\gamma}^{(D)} = \frac{1}{N^{(D)}} \sum_{p'=0}^{N^{(D)}-1} \gamma_{p'}^{(D)} \geq \gamma^t$. Here, γ^t denotes the SINR threshold required for successful demodulation of the TV signal. Similarly, $\bar{\gamma}^{(U)} = \frac{1}{N^{(D)}} \sum_{p'=0}^{N^{(D)}-1} \gamma_{p'}^{(U)} \geq \gamma^t$ represents mean SINR of TV signal at the IC module of UAV-Rx [12]. The proposed AMDS framework is based on the UAV-Tx dynamically adapting the level of modulation format (bit loading ($x \in \chi$)) and number of subcarriers ($F \in \{1, 2, \ldots, N^{(U)}\}$) to maximize the throughput in addition to controlling the interference over the TV-Rx. The transmit power is selected to ensure that the channel averaged bit error probability (ABEP) of the UAV signal (M-QAM symbol transmitted at bit loading of $x = \log_2 M$), denoted as $\rho(\Gamma^{(U)}, 2^{(x)})$, received at the UAV-Rx with average SINR of Γ_p^U, remains below a predefined threshold ϵ.

$$\begin{aligned}
\text{(P1)}: \quad & \max_{F, x, P^{(U)}} \quad \frac{F \cdot x}{T^{(U)}} \\
\text{s.t.,} \quad & (C1): \bar{\gamma}^{(D)} \geq \gamma^t, (C2): \bar{\gamma}^{(U)} \geq \gamma^t \\
& (C3): F \cdot P^{(U)} \leq P_m^{(G)} \\
& (C4): \rho(\Gamma_p^{(U)}, 2^x) \leq \epsilon \ \forall \ x \in \chi, p = \{0, 1, \ldots, F-1\} \\
& (C5): F \in \{1, 2, \ldots, N^{(G)}\}, (C6): x \in \chi.
\end{aligned}$$

Here, The objective of the problem (P1) represents the throughput of the UAV network over $T^{(U)}$ duration. The constraint $(C1)$ protects the QoS of the TV-Rx, as the UAV network coexists with the DTV network. Constraint $(C2)$ ensures perfect IC at the UAV receiver. $(C3)$ constraints the UAV power budget. Constraint $(C4)$ ensures that the UAV transmit power $(P^{(U)})$ and bit loading x are chosen such that the ABEP of the received symbol is less than threshold ϵ. For M-QAM modulation formats, the ABEP expression in the Rayleigh fading channel is provided in [13, Eq. (8.111)]. The constraint $(C5)$ restricts the UAV subcarriers to the feasible set, while constraint $(C6)$ ensures the bit loading is selected from the available set only. The constraint $(C1)$, $(C2)$, and $(C4)$ are non-linear in terms of the optimization variables, and the variables F and x are integral constraints. Therefore, the problem $(P1)$ is an integer non-linear program. We discuss the solution of problem $(P1)$ in the upcoming subsection.

A. Proposed solution

We present an adaptive modulation and dynamic subcarrier (AMDS) framework to solve the problem $(P1)$. The constraint $(C4)$ can be relaxed by pre-computing $P^{(U)}$ for each available modulation format by solving the equation $(\rho(\Gamma^{(U)}, 2^{(b_i)}) = \epsilon)$. This is a non-linear equation that can be solved using the trust-region-dogleg algorithm [14] in MATLAB. Let $P^{(U)}[i]$ denote the power obtained for loading b_i bits per symbol obtained in the previous step. For fixed x the objective of problem $(P1)$ is monotonically increasing in variable F. Therefore, for a fixed bit loading the optimal number of subcarriers can be determined by solving equation $\bar{\gamma}(F) \geq \gamma^t$, where $\gamma(F) = \min[\bar{\gamma}^{(D)}, \bar{\gamma}^{(U)}]$. Due to the monotonically decreasing nature of the equation in variable F, the equation can be solved using the bisection search algorithm. The overall steps for solving problem $(P1)$ are present in the AMDS algorithm 1. The worst-case complexity of the overall algorithm is given by $|\chi| \cdot \mathcal{O}(\log(N^{(U)}))$, where $|\chi|$ denote the cardinality of the set.

V. Results and Discussion

The parameters used for simulations are shown in Table I. For the simulations, we have considered TV-Tx, UAV-Tx, TV-Rx, and UAV-Rx to be co-linear as shown in Fig. 1. We have assumed typical urban 6 (TU-6) multipath channel for TV signal. For simulations, the OFDM waveforms of UAV-Tx are assumed similar to ATSC 3.0 waveform. The heights of TV-Tx ($h_t^{(D)}$) and TV-Rx ($h_r^{(D)}$) are assumed to be fixed at

Algorithm 1: Proposed adaptive modulation and dynamic subcarrier framework

for $i \in |\chi|$ **do**
  $P^{(U)}[i] \leftarrow solve(\rho(\Gamma^{(U)}, 2^{(b_i)}) = \epsilon)$;
  $LW \leftarrow 1$; $UP \leftarrow 1$;
  if $\bar{\gamma}(LW) - \gamma^t) \cdot (\bar{\gamma}(UP) - \gamma^t) \leq 0$ **then**
    while $LW + 1 < UP$ **do**
      $t = \lfloor (LW + UP)/2 \rfloor$;
      if $\gamma(t) \geq \gamma^t$ **then**
        $LW \leftarrow t$
      else
        $UP \leftarrow t$;
      end
    end
    if $\gamma(LW) \geq 0$ **then**
      $F[i] \leftarrow LW$
    else
      $F[i] \leftarrow UP$
    end
  else
    if $\bar{\gamma}(LW) - \gamma^t) \cdot (\bar{\gamma}(UP) - \gamma^t) > 0$ **then**
      if $\bar{\gamma}(LW) < \gamma^t$ **then**
        $F[i] = 0$;
      else
        $F[i] = UP$;
      end
      L
    end
  end
end
$i_{max} = \text{argmax}(F)$ and **Return** $F = F[i_{max}], x = b[i_{max}]$;

Table I: Simulation Parameters

	ATSC 3.0	UAV-Tx
Bandwidth	6 MHz	6 MHz
Transmit power	4 kW	10 W
Sub-carrier spacing	843 Hz	843 kHz
OFDM Useful symbol duration	1186 μs	1186 μs
OFDM guard	148.15 μs	148.15 μs
Active Subcarriers	6913	6913
Path loss exponent	Urban Hata	3GPP rel. 18

350 m and 5 m, respectively. The values of carrier frequency, noise PSD (N_0), and ABEP threshold (ϵ) are 605 MHz, -166dBm/Hz, and and 10^{-3}, respectively.

A. Effect of UAV-Rx motion on the throughput of the UAV link

The scenario considers a fixed horizontal distance of 500 m between the UAV-Tx and the TV-Rx (d_1), with the UAVs operating at a height of 10 m above the ground. Fig 2 (a) shows the variation of UAV throughput with the distance between the TV-Rx and UAV-Rx (d_2). It is observed that for $d_{TV} = 10$ km, as d_2 increases, the throughput of the UAV link decreases. This is due to increasing path loss with increasing d_2, requiring more power to satisfy the BER constraint. Consequently, the UAV-Tx reduces the subcarrier allocations to compensate for the increased interference at the TV-Rx as inferred from Fig 2 (a). However, the UAV-Tx does not change the modulation scheme as can be observed from Fig 2 (b). At $d_{TV} = 35$ km, the throughput decreases with increasing d_2. In this case, till $d_2 \leq 750$ m, the proposed AMDS scheme compensates for the increase in interference by reducing the allocated subcarriers as seen in Fig 2 (a). Beyond $d_2 > 750$ m, the proposed AMDS scheme compensates the interference by reducing the modulation format level to 64-QAM as can be seen in Fig 2 (b), thereby causing less interference to the TV-Rx. Lowering the modulation scheme provides room to the AMDS scheme to allocate more subcarriers which explains the increase in the number of assigned subcarriers at $d_2 = 1$ km in the Fig 2 (a).

The effect of variation of the UAV-Rx height on the throughput of the UAV link is depicted in Fig 2 (c). The scenario considers $d_1 = d_2 = 500$ m. The UAV transmitter is flying at a height of 10 m above the ground while the height of the UAV receiver is variable. Similar to the observations made in the horizontal motion case, the throughput of the UAV link decreases as the height of the UAV-Rx increases due to the increasing distance between the UAV-Tx and UAV-Rx. This degradation in throughput is caused by the same factors discussed in the previous paragraph.

B. Effect of UAV-Tx motion on UAV link throughput

The scenario considers a fixed horizontal distance of 500 m between the UAV-Rx and TV-Rx (d_2). Fig 3 (a) shows the variation of UAV throughput with the distance between the TV-Tx and the UAV receiver (d_1). It can be seen that the UAV link throughput increases as distance d_1 increases. This is because of the increased physical distance between the UAV-Tx and the TV-Rx (thus the TV-Rx is less prone to interference), resulting in the UAV-Tx to transmit data with more subcarriers and higher modulation format as depicted in Figs 3 (a) and (b), respectively.

The variation of UAV link throughput with variation in the height of the UAV-Tx is shown in Fig 3 (c). The simulation is performed at $d_1 = d_2 = 500m$. The UAV-Rx is flying at a fixed height of 10 m above the ground while the height of UAV-Tx is variable. It can be seen that the throughput of the UAV link increases as the height of UAV-Tx increases this is due to the increase in distance between UAV-Tx and TV-Rx. This improvement in throughput is caused by the same factors discussed in the previous paragraph.

For the same relative distances between UAV-Tx, TV-Rx, and UAV-Rx, the throughput of UAV link decreases as the TV-Rx moves away from the TV-Tx. This is due to the reduced TV signal strength, consequently lowering the interference margin at the TV-Rx. Therefore, the proposed AMDS strategy reduces the UAV throughput to maintain the QoS of TV-Rx, as observed from Figs. 2 (a), (c) and Figs. 3 (a), (c).

Remark 1. *The proposed AMDS framework is highly effective in coexisting the UAV network in DTV bands. The coexisting UAVs can achieve a capacity of around 40 Mbps, when they are up to 1 km apart from each other, in addition to protecting the performance of TV receiver.*

Remark 2. *It is inferred that the UAV network capacity increases when the UAV-Tx moves away (horizontally or vertically) from UAV-Rx. On the contrary, the UAV network capacity decreases when the UAV-Rx. moves away from UAV-Tx. This asymmetric behaviour is due to the presence of TV receiver and the proposed AMDS framework protecting its QoS from the resulting coexisting interference.*

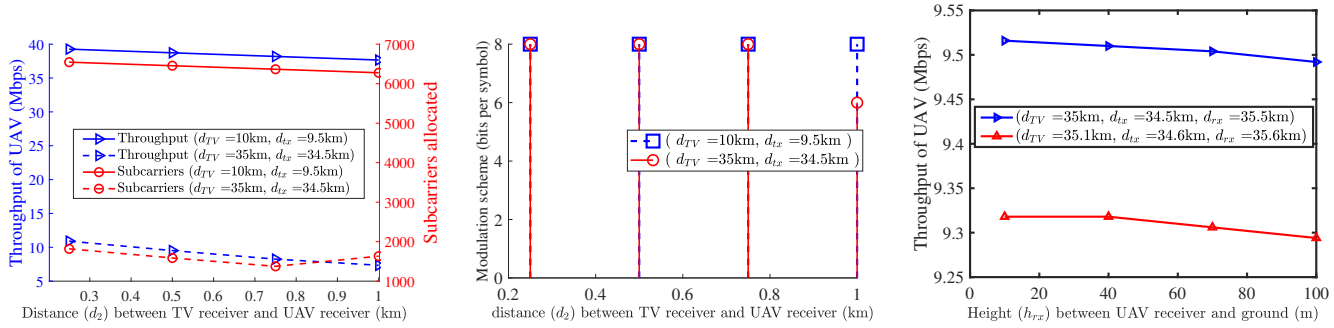

(a) (b) (c)

Figure 2: Variation of (a) UAV link throughput and the number of allocated subcarriers with the horizontal motion of UAV-Rx. (b) modulation scheme assignment with the horizontal motion of UAV-Rx. (c) UAV link throughput with the vertical motion of the UAV-Rx.

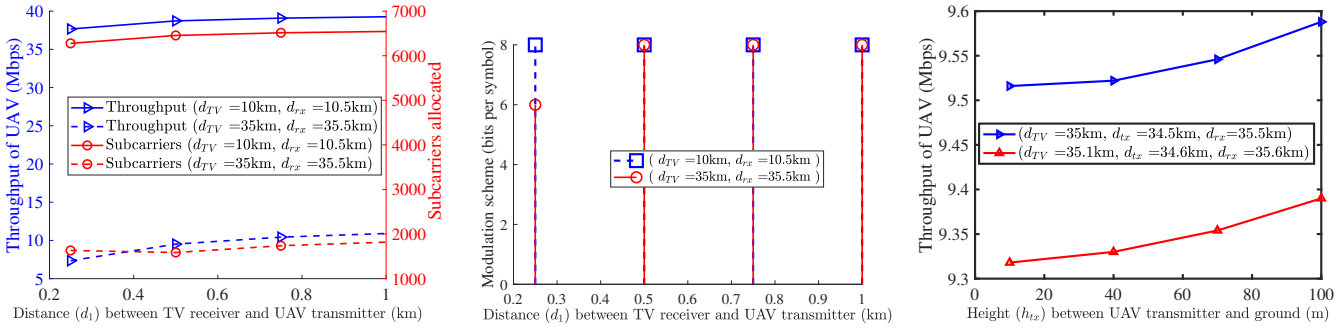

(a) (b) (c)

Figure 3: Variation of (a) UAV link throughput and the number of allocated subcarriers with the horizontal motion of UAV-Tx. (b) modulation scheme assignment with the horizontal motion of UAV-Tx. (c) UAV link throughput with the vertical motion of the UAV-Tx.

VI. Conclusion

This work has studied and demonstrated the feasibility of coexisting UAV based communication networks over DTV bands. The resource allocation of the UAV network has been performed intelligently through the proposed adaptive bit loading and frequency allocations based AMDS framework. In this regard, a network rate maximization problem has been formulated. The problem has been solved using bi-section method, which has been observed to have lower computation complexity over the traditional exhaustive search method. The proposed method is expected to aid in developing spectrum sharing techniques for designing upcoming future networks.

Acknowledgement

This work was supported in parts by the Indian National Academy of Engineering (INAE) through the Abdul Kalam Technology Innovation National Fellowship, the Tehri Hydroelectric Development Corporation under Grant THDC/RKSH/R&D/F-2076/1036, the Science and Engineering Board under Grant CRG/2023/005421, and the Prime Minister's Research Fellows scheme.

References

[1] W. Zhang *et al.*, "Enhanced 5G cognitive radio networks based on spectrum sharing and spectrum aggregation," *IEEE Trans. Commun.*, vol. 66, no. 12, pp. 6304–6316, 2018.

[2] P. Ameigeiras *et al.*, "Dynamic deployment of small cells in TV white spaces," *IEEE Trans. Veh. Technol.*, vol. 64, no. 9, pp. 4063–4073, 2015.

[3] M. Mozaffari *et al.*, "A tutorial on UAVs for wireless networks: Applications, challenges, and open problems," *IEEE Commun. Surv. Tut.*, vol. 21, no. 3, pp. 2334–2360, 2019.

[4] J. Sachs *et al.*, "Cognitive cellular systems within the TV spectrum," in *DySPAN*, 2010, pp. 1–12.

[5] A. Thakur *et al.*, "Co-channel secondary deployment over DTV bands using reconfigurable radios," *IEEE Trans. Veh. Technol.*, vol. 69, no. 10, pp. 12 202–12 215, 2020.

[6] L. Polak *et al.*, "Coexistence between DVB-T/T2 and LTE standards in common frequency bands," *Wirel. Pers. Commun.*, vol. 88, no. 3, p. 669–684, jun 2016.

[7] H. Bawab *et al.*, "Spectral overlap optimization for DVB-T2 and LTE coexistence," *IEEE Trans. Broadcast.*, vol. 64, no. 1, pp. 70–84, 2018.

[8] R. Dubey and S. De, "SIC based secondary coexistence over ATSC 3.0 broadcast channels," in *IEEE MILCOM*, 2022, pp. 751–756.

[9] L. Fay *et al.*, "An overview of the ATSC 3.0 physical layer specification," *IEEE Trans. Broadcast.*, vol. 62, no. 1, pp. 159–171, 2016.

[10] A. Balakrishnan, S. De, and L.-C. Wang, "HAPS-aided power grid connected green communication framework: Architecture and optimization," in *IEEE ICC*, 2024, pp. 2847–2852.

[11] X. Zhou *et al.*, "Energy-efficient power loading with intercarrier and intersymbol interference considerations for cognitive OFDM systems," in *Proc. VTC Spring*, 2015, pp. 1–5.

[12] A. Balakrishnan *et al.*, "CASE: A joint traffic and energy optimization framework toward grid connected green future networks," *IEEE Trans. Netw. Serv. Manag.*, vol. 21, no. 3, pp. 2888–2899, 2024.

[13] *Digital Communication over Fading Channels*. John Wiley & Sons, Ltd, Nov. 2004, ch. 8, pp. 223–309.

[14] M. J. Powell, "A fortran subroutine for solving systems of nonlinear algebraic equations." [Online]. Available: https://www.osti.gov/biblio/4772677